学位論文

Anti-fibrotic effect of lysophosphatidic acid receptors LPA_1 and LPA_3 antagonist on experimental murine scleroderma induced by bleomycin

（ブレオマイシン誘導性皮膚硬化モデルマウスにおけるリゾホスファチジン酸受容体（$LPA_{1,3}$）拮抗薬の抗線維化効果）

福島県立医科大学大学院医学教育学部博士課程医学専攻皮膚粘膜学

大橋　威信

概要

全身性強皮症（systemic sclerosis:SSc）は、皮膚、肺を含む様々な臓器に線維化をきたす結合織疾患である。線維化の機序はまだ十分明らかになっておらず、現在のところ有効な治療法も少ない。近年、リソホスファチジン酸（lysophosphatidic acid :LPA)が臓器線維化において重要な働きがあるとして注目されている。LPA は G 蛋白質共役型受容体（GPCR）を介し，多彩な機能を発揮する生理活性脂質である。近年、ヒト強皮症の血清中や皮膚線維芽細胞で LPA の発現が亢進していることが報告された。また、皮膚や肺、腎を含む線維症モデルにおいても、LPA_1 受容体欠損により線維化の誘導が抑制されており、LPA は高親和性 LPA_1 受容体を介して線維化を誘導する重要なメディエーターであることが明らかにされた。その役割として線維芽細胞の運動促進活性や、種々の細胞において炎症性サイトカインの発現誘導活性を持ち、炎症や組織修復に機能することが示唆されている。

本研究では、ブレオマイシン誘導性強皮症モデルマウスを用いて、$LPA_{1,\ 3}$ 受容体拮抗薬（Ki16425）を局所投与し、皮膚硬化および肺線維化に与える影響について検討した。C3H/HeJ マウス（6 週令、雌）の背部にブレオマイシン（250 μg/ml）を 100 μl 皮内注射し、Ki16425 の濃度を 1mg/kg、10mg/kg となるように調節し、6 時間後に同部位に 100 μl 皮内注射した。週 5 回 4 週間投与した後、6mm パンチで背部の BLM 注射部位の皮膚および肺組織を採取し、病理組織学的、生化学的、遺伝子学的な検討を行った。

真皮厚はコントロール群と比較して、Ki16425 (1mg/kg)群では 38%、Ki16425 (10mg/kg)群では 35%減少しており、組織学的な皮膚硬化の抑制がみられた。膠原線維束の肥厚には、Ki16425 の濃度の違いによる有意差は認められなかった。皮膚のヒドロキシプロリン量はコントール群に比べて、Ki16425 (1mg/kg)群では 32%、Ki16425 (10mg/kg)群では 49%の減少が認められた。真皮内で肥満細胞数は Ki16425 投与により、有意に減少してみられた。真皮内の α-SMA 陽性筋線維芽細胞数は Ki16425 投与により有意に減少していた。さらに、p-Smad 2/3 陽性細胞数は Ki16425 投与群で有意に減少していた。皮膚組織を用いた realtime-PCR の検討では、ブレオマイシン処理された皮膚局所における TGF-β1、CTGF、MIP-1α、IFN-γ、collagen α1(I) mRNA の発現レベルが Ki16425 投与により有意に抑制されていた。肺組織においては、肺胞壁の浮腫を伴う肥厚の減少、炎症細胞浸潤の減少を認め、肺線維スコアでも有意に減少していた。肺組織中のヒドロキシプロリン量はコントロール群に比べて減少する傾向が認められた。

以上より、$LPA_{1,\ 3}$ 受容体拮抗薬である Ki16425 はブレオマイシン誘導性強皮症モデルマウスにおいて皮膚および肺の線維化を改善させることが示唆された。これらの結果は、SSc に対する新しい抗線維化薬としての Ki16425 の可能性を示唆するとともに、SSc における線維化に対する今後の治療戦略を考える上で重要な知見と考えられる。

abbreviation

SSc: Systemic sclerosis:

LPA: lysophosphatidic acid

TGF- β: transforming growth factor-β1

CTGF: connective tissue growth factor

IL-4: interleukin-4

MCP-1: monocyte chemotactic protein-1

GPCRs: G-protein-coupled receptors

lysoPLD: lysophospholipase D

PBS: phosphate-buffered saline

H&E: hematoxylin and eosin

MIP-1α: macrophage inflammatory protein-1α

IFN-γ: interferon-γ

TNF-α: tumor necrosis factor-α

mRNA: messenger RNA

HPF: high-power field

JNK: c-jun N-terminal kinase

ERK: extracellular signal-regulated kinase

Introduction

Systemic sclerosis (SSc) is a multiorgan connective tissue disease with variable rate of mortality and morbidity. Fibrogenetic pathogenesis in SSc is due to impaired vasculopathy, systemic autoimmunity, and fibrosis, which lead to tissue fibrosis (1). The mechanisms are complex and multiple fibrogenic mediators have been detected in SSc, including transforming growth factor-β1 (TGF-β1) and -β2, connective tissue growth factor (CTGF), tryptase, interleukin-4 (IL-4), IL-6, IL-13, IL-17, and monocyte chemotactic protein-1 (MCP-1) (2-6). A recent study found that lysophosphatidic acid (LPA) is involved and plays an important role in the pathogenesis of SSc (7). LPA is a lipid mediator that signals through specific G-protein-coupled receptors (GPCRs), designated as LPA_1 to LPA_8 (8-9). In serum, activated platelets are mainly the primary source of LPA, which is produced by the action of lysophospholipase D (lysoPLD), also known as autotaxin, on lysophosphatidylcholine (LPC) and other lysophospholipids (10). LPA exerts various physiological effects on receptors of parenchymal cells. LPA has been reported to be associated with the pathogenesis of SSc, which shows that LPA levels are elevated in serum of SSc compared with serum of healthy controls (11), fibroblasts cultured from SSc skin showed a significant increase of LPA-activated chloride channel current activity following LPA exposure compared with control skin fibroblasts (12). Also, role of LPA has been demonstrated in several animal model systems including skin fibrosis, pulmonary fibrosis, liver fibrosis, and renal fibrosis (13-17). In a renal fibrosis model, tubulointerstitial fibrosis was reduced in LPA_1 receptor knockout mice by unilateral ureteral obstruction (16). In the same study, the $LPA_{1,3}$ receptor antagonist significantly reduced in renal fibrosis and decreased TGF-β and CTGF mRNA expression (16). The investigations suggest that LPA_1 and/or LPA_3

play an upstream role of these fibrogenic mediators in the pathogenesis of SSc.

In the present study, we assessed the efficacy of LPA_1 and LPA_3 receptor antagonist Ki16425 (3-[[[4-[4-[[[1-(2-chlorophenyl)ethoxy]carbonyl]amino]-3-methyl-5-isoxazoly]phenyl]methyl]thio]-propanoic acid) in a mouse model of scleroderma induced by bleomycin. This model is widely used because skin fibrosis and lung fibrosis resembling scleroderma can be produced by repeated local injections of bleomycin (18, 19). Although a variety of factors have been reported to contribute to the fibrotic process in the bleomycin-induced mouse as a scleroderma model, which showed collagen deposition and both fibroblast and myofibroblast accumulation in the dermis of this model (20), lesional skin also shows increased Smad 2 and Smad 3 phosphorylation (21), indicating activation of the TGF-β pathway for inducing to scleroderma (22, 23). We focused on the fibrogenic function of LPA in scleroderma and examined the potential benefit of local LPA_1 and LPA_3 receptor antagonist administration in the mouse scleroderma induced by bleomycin.

Materials and methods

Animals and reagents

Specific, pathogen-free C3H-HeJ female mice (six weeks old) weighing 20 g were purchased from CLEA Japan, Inc. (Tokyo, Japan) and housed in a controlled environment (21-24 °C, 60 % humidity, 12 h light/dark cycle). The mice were kept in a separate, clean room in our animal facility and fed ad libitum. Three to seven mice were used in the experiment. All experimental procedures in this study were approved by the Animal Care Committee of Fukushima Medical University.

Bleomycin-induced scleroderma model mice

The scleroderma mouse model was established according to our previous methods (18). Bleomycin (Nippon Kayaku Co., Ltd., Tokyo) was dissolved in phosphate-buffered saline (PBS) at a final concentration of 250 μg/ml. After filter sterilization, 100 μl of bleomycin was intradermally injected into the shaved back of the mice once daily for five days/week for four weeks.

Ki16425 treatment

Ki16425 (Santa Cruz Biotechnology, Inc., Texas, USA) powder was diluted in sesame oil (Sigma-Aldrich, St. Louis, MO, USA) at a concentration of 200 μg/ml or 2 mg/ml and then 100 μl of the solution was administered (approximately the dose of 1 mg/kg/day or 10 mg/kg/day). Ki16425 was administered by intradermal injection after 6 h on the same site with bleomycin injection once daily for five days/week for four weeks.

Histopathological analysis of dermal fibrosis and dermal thickness measurement

The injected skin sites were punch biopsied (6 mm) and cut into two pieces. One was used for paraffin-embedded sectioning into multiple 5 μm sections, which were deparaffinized, rehydrated, and stained with hematoxylin and eosin (H&E) or Elastica-Masson. The other was stored immediately in liquid nitrogen for cryosectioning. For evaluation of skin sclerosis, and determination of dermal thickness with the use of photomicrographs (magnification × 100) of H&E-stained sections, measuring the distance between the epidermal-dermal junction and the

dermal-fat junction at ten randomly selected sites per section. Infiltrating mast cells in the dermis were characterized by toluidine blue staining, counted in ten distinct fields under a light microscope at a magnification of × 400 and then expressed as mean cell numbers ± SD.

Histopathological assessment of lung fibrosis

After a four-week treatment with Ki16425, lungs were excised from the bleomycin-induced mice. Lung tissue was stained using H&E and Elastica-Masson and the severity of lung fibrosis was determined by semiquantitative histopathological scoring using light microscopy (magnification × 100). To do this, lung fibrosis was scored on a scale of 0-8 by examining 45 randomly chosen fields (5 lobes/mouse × 3 sections/lobe × 3 fields/section) for each mouse. As defined by Ashcroft et al. (24), the criteria for grading lung fibrosis were as follows: grade 0 = normal lung; grade 1 = minimal fibrous thickening of alveolar or bronchiolar walls; grade 3 = moderate thickening of walls without obvious damage to lung architecture; grade 5 = increased fibrosis with definite damage to lung structure and formation of fibrosis with definite damage to lung structure and formation of fibrous bands or small fibrous masses masses; grade 7 = severe distortion of structure and large fibrous areas; and grade 8 = total fibrosis obliteration of the fields.

Immunohistochemical staining

Multiple 5 μm sections of paraffin-embedded skin samples were deparaffinized and rehydrated. Immunolabeling of α-smooth muscle actin (α-SMA) and phospho-Smad 2/3 was performed by detection with an avidin-biotion-peroxidase complex with

primary rabbit anti–mouse α-SMA antibody (Abcam, Tokyo) and primary goat anti–mouse phospho-Smad 2/3 antibody (Santa Cruz Biotechnology, Inc.). Ten randomly selected stain-positive cells were counted in dermal sections under a light microscope at a magnification of × 400.

Hydroxyproline assay in the skin and lung tissue

Hydroxyproline content was determined by measuring biopsied skin and lung collagen. The ground skins and lungs were dried for 20 h in a 110°C incubator. Then, they were hydrolyzed in 6N hydrochloric acid at 110°C for 24 h. After neutralizing with appropriate amounts of 6N sodium hydroxide, the hydrolysates were diluted with distilled water. The hydrolysates were then mixed after adding 2 g KCl and kept on ice for 15 min. The mixture was oxidized with 1.0 ml of 0.2 M chloramine-T solution and kept on ice for 120 min. The oxidation reaction was stopped by adding 2 ml of 3.6 M sodium thiosulfate in boiling water for 30 min. After cooling to room temperature, the product was mixed with 2.0 ml toluene and centrifuged at 300–400 *g* for 5 min to separate the pyrrole reaction product. The final pyrrole reaction product contained in 2.0 ml of the toluene layer was mixed with 0.8 ml of Ehrlich's reagent and was measured against hydroxyproline standards at 650 and 562 nm. Hydroxyproline contents were given per 100 μl volume of the hydrolysate.

RNA isolation and RT-PCR

Total RNA was extracted from frozen skin tissue using ISOGEN (NIPPON GENE, Tokyo) and was treated with DNase (TURBO DNase Kit; Applied Biosystems, Carlsbad, CA, USA) followed by reverse transcription to synthesize single-strand cDNA with

random hexamers (High Capacity RNA-to-cDNA Kit, Applied Biosystems). Serial dilution of the cDNA obtained was cycle-amplified specifically with specific primer sets for TGF-β1, CTGF, macrophage inflammatory protein-1α (MIP-1α), interferon-γ (IFN-γ), tumor necrosis factor-α (TNF-α), and collagen α1 (I). GAPDH was used to normalize messenger RNA (mRNA) expression. All primers used were designed using the Perfect Real Time support system (Takara Bio, Shiga, Japan) (Table. 1). The PCR mixture contained 2 μl (serially equating 0.2–200 ng/μl) cDNA, 7 μl DNase, 10× PCR SYBR Green Master mix (Applied Biosystems), and oligonucleotide primer sets in a volume of 25 μl of nuclease-free water. PCR was carried out under a logarithmic phase of amplification as follows: 95°C for 5 min followed by 40 cycles of amplification; 95°C for 30 s, 58°C for 30 s, and 72°C for 30 s using the ABI StepOne system (Applied Biosystems).

Statistical analysis

All of the data were expressed as mean ± SD and analyzed using StatView software (version 5.0; SAS Institute Inc., Cary, NC, USA). Differences between Ki16425-treated and Ki16425-untreated mice in the median value of each parameter were evaluated by an unpaired Mann-Whitney U test. $p < 0.05$ was considered statistically significant.

Results

Local injection of $LPA_{1,3}$ receptor antagonist Ki16425 inhibits the dermal sclerosis induced by bleomycin treatment

On examination of H&E staining, the skin injected with bleomycin and sesame oil as a

control had strikingly induced dermal sclerosis. By compassing the bleomycin-Ki16425-injected skin sites showed marked decreases of dermal sclerosis compared with the bleomycin-oil-injected skin sites (Fig. 1a-c). Regarding the histology of injected skin sites of the oil-treated mice, the Ki16425-treated mice revealed thickening of the dermal collagen bundles and decreased deposition of collagen fibers, as assessed by Elastica-Masson's staining (Fig. 1d-f). We next assessed the dermal thickness of the control mice and Ki16425-treated mice. Compared with findings in bleomycin-oil-treated mice, Ki16425 decreased dermal thickness by 38% in Ki16425-treated mice dosed with 1 mg/kg, and 35% in Ki16425-treated mice dosed with 10 mg/kg (Ki16425 (1 mg/kg): 134.7 ± 18.57 μm vs oil: 217.5 ± 16.72 μm, $p < 0.05$; Ki16425 (10 mg/kg): 142.7 ± 12.51 μm vs oil: 217.5 ± 16.72 μm, $p < 0.05$). However, there was no statistically significant dose dependence of Ki16425-induced inhibition (Fig. 1g). We assessed biochemically skin collagen by measuring hydroxyproline content. The levels of hydroxyproline in the Ki16425-injected skin sites showed a significant decrease of 32% (1 mg/kg) and 49% (10 mg/kg) compared with the control oil injection (Ki16425 (1 mg/kg): 23.76 ± 1.11 μg/ml vs oil: 35.05 ± 0.83 μg/ml, $p < 0.05$; Ki16425 (10 mg/kg): 17.72 ± 8.22 μg/ml vs oil: 35.05 ± 0.83 μm, $p < 0.05$) (Fig. 1h).

$LPA_{1,3}$ receptor antagonist injection reduces mast cell infiltration in bleomycin-induced scleroderma skin

After four weeks of bleomycin injection, intradermal infiltration of mast cells into the injected skin sites was dramatically increased, as assessed by toluidine blue staining (Fig. 2a-c). The number of mast cells of Ki16425-treated skin sites was significantly

decreased compared with the skin treated with oil (Ki16425 (1 mg/kg): 97.2 ± 14.09/10 high-power field (HPF) vs oil: 139.8 ± 8.23/10 HPF, $p < 0.05$; Ki16425 (10 mg/kg): 82.0 ± 7.67/10 HPF vs oil: 97.2 ± 14.09/10 HPF, $p < 0.05$). However, the Ki16425 dose did not significantly affect the number of infiltrating mast cells (Fig. 2d).

$LPA_{1,3}$ receptor antagonist injection reduces myofibroblast accumulation in bleomycin-induced scleroderma skin

We compared the number of α-SMA-positive myofibroblasts in the dermis of Ki16425-injected mice and control mice. Myofibroblasts in the dermis were decreased in the Ki16425-treated mice (Fig. 3a-c). For quantification, the number of α-SMA–positive myofibroblasts in the dermis of the Ki16425-treated mice was significantly decreased compared with the control mice (Ki16425 (1 mg/kg): 82.4 ± 14.26/10 HPF vs oil: 121.0 ± 4.69/10 HPF, $p < 0.05$; Ki16425 (10 mg/kg): 75.8.0 ± 7.96/10 HPF vs oil: 121.0 ± 4.69/10 HPF, $p < 0.05$) (Fig. 3d). However, there was no significant dose dependency of inhibition in the Ki16425-treated group.

$LPA_{1,3}$ receptor antagonist injection reduced phospho-Smad 2/3 expression of fibroblasts in the bleomycin-induced mice

To examine the phosphorylation status of receptor-regulated Smad in dermal cells using a specific antibody that recognizes phosphorylated Smad 2 and Smad 3, we compared the number of cells with nuclear Smad 2/3 phosphorylation in the dermis of bleomycin-injected control and Ki16425-treated mice. Bleomycin injection increased the number of nuclear phospho-Smad 2/3–positive cells in the dermis of the control mice, whereas Ki16425 treatment decreased the number of phospho-Smad 2/3–positive

cells in the dermis (Fig. 4a-c). For quantification, the number of phospho-Smad 2/3–positive cells in the dermis of Ki16425-treated mice was counted, what was significantly decreased compared with that in the dermis of the control mice (Ki16425 (1 mg/kg): 23.5 ± 4.88/10 HPF vs oil: 31.6.0 ± 4.67/10 HPF, $p < 0.05$; Ki16425 (10 mg/kg): 21.9 ± 2.98/10 HPF vs oil: 31.6 ± 4.67/10 HPF, $p < 0.05$) (Fig. 4d). However, there was no significant dose dependency of inhibition in the Ki16425-treated group.

$LPA_{1,3}$ receptor antagonist reduces fibrogenic cytokines and collagen α1(I) mRNA expression induced by bleomycin

Transcriptional levels of TGF-β1, CTGF, MIP-1α, IFN-γ, and TNF-α, which are important cytokines involved in fibrogenesis, were analyzed by a real-time PCR assay. The expression of TGF-β1, CTGF, and MIP-1α mRNA was significantly decreased in both the 1 mg/kg and 10 mg/kg groups of Ki16425-treated mice compared with the mice treated with sesame oil as a control. The dose of 10 mg/kg Ki16425 treatment revealed a significant decrease in expression levels of IFN-γ and collagen α1 (I) mRNA compared with the control groups. The Ki16425 1 mg/kg dose treatment had no significant effects, however tended to reduce IFN-γ ($p = 0.119924$) and collagen α1 (I) mRNA expression ($p = 0.183473$). A significant difference was not observed between the control groups and Ki16425-treatment groups regarding TNF-α mRNA expression, which tended to be increased slightly in the Ki16425-treatment groups (Fig. 5).

$LPA_{1,3}$ receptor antagonist inhibits the induction of lung fibrosis in bleomycin-induced lung injury

Histopathological examination of lungs of the mice with induced scleroderma by local

intradermally injected bleomycin revealed significant damage to the lung tissue, including thickening of the alveolar septae, alveolar inflammation, and fibrous obliteration of the peribronchiolar and parenchymal regions. The lung tisuue of bleomycin-Ki16425-injected mice showed marked decreases of damage compared with the lung tissue of bleomycin-oil-injected mice (Fig. 6a-c). The reduction in fibrosis was confirmed by quantitative analysis of histological scoring of lung fibrosis (Ki16425 (1 mg/kg): 3.0± 0.89 μg/ml vs control: 4.6 ± 1.02 μg/ml, $p < 0.05$; Ki16425 (10 mg/kg): 2.6 ± 0.80 μg/ml vs control: 4.6 ± 1.02 μm, $p < 0.05$) (Fig. 6d).

$LPA_{1\,3}$ receptor antagonist injection reduces hydroxyproline contents in the lung

We measured collagen contents of the lung of mice treated with bleomycin and Ki16425 for four weeks. The levels of hydroxyproline of the lung in Ki16425-treated mice showed a significant decrease of 25% (1 mg/kg) and 32% (10 mg/kg) compared with the control oil injection (Ki16425 (1 mg/kg): 25.77 ± 6.03 μg/ml vs control: 34.54 ± 6.51 μg/ml, $p < 0.05$; Ki16425 (10 mg/kg): 23.56 ± 6.61 μg/ml vs control: 34.54 ± 6.51 μm, $p < 0.05$) (Fig. 6e).

Discussion

The present study have shown that 1) bleomycin-induced dermal sclerosis was inhibited by local injection of $LPA_{1,3}$ receptor antagonist Ki16425 on the same site with bleomycin injection, 2) Ki16245 reduced the expression of fibrogenic cytokines, TGF-β_1, CTGF, and the numbers of mast cells and myofibroblasts in the dermis, 3) lung fibrosis was reduced by Ki16425 local injection on the bleomycin-induced scleroderma model. These observations strongly suggest the effectivity of $LPA_{1,3}$ receptor antagonist

in skin and lung fibrosis, implicating that the LPA_1 receptor may represent a potential of a pharmaceutical target for the treatment of SSc.

LPA is a growth factor–like phospholipid known to regulate several cellular processes via the activation of specific G protein–coupled receptors ($LPA_{1–8}$) (8, 9) and has been shown to promote wound healing in multiple tissues, including the skin in humans and mice (25, 26). LPA levels were recently noted to be significantly higher in the serum of SSc patients as compared with healthy controls (11). The fibrogenic role of the LPA_1 receptor has been revealed in the skin, lung, kidney, and liver animal models. In addition, administration of the $LPA_{1,3}$-receptor-selective antagonist Ki16425 reduced kidney fibrosis. Thus, this and other studies have highlighted the role of LPA signaling in fibrotic disease and have identified the LPA_1 receptor as a therapeutic target for treating skin fibrosis. For this reason, we demonstrated a novel $LPA_{1,3}$ receptor antagonist Ki16425 which inhibits fibrosis in skin and lung by experiments using the bleomycin model mouse. Furthermore, we evaluated the potential of Ki16425 as a treatment for SSc. Several possible explanations could account for the hypothesis of $LPA_{1,3}$ receptor antagonist Ki16425's effect on the processes in dermal and lung fibrosis in the bleomycin-induced mice. The assumable mechanisms are through 1) TGF-β/Smad signaling pathway activation, 2) myofibroblasts accumulation, and 3) mast cells infiltration.

Normal fibroblasts transdifferentiate into myofibroblasts under the influence of TGF-β (27). In a normal cell, TGF-β signaling leads to phosphorylation and activation of receptor-regulated Smad2 and Smad3 (28), nuclear accumulation and phosphorylation of Smad 2/3 are constituted in scleroderma fibroblasts (29). In a bleomycin-induced SSc mouse model, Smad3 and phospho-Smad2/3 expression are

increased in dermal fibroblasts, and Smad 2/3 nuclear localization and phosphorylation show evidence of sustained stimulation of TGF-β-regulated genes (22). A key player in fibrosis is TGF-β, which has been shown to be of paramount importance in both SSc patients (30) and mouse models (31, 32). TGF-β's contribution to fibrosis via the activation of increased levels of TGF-β receptors on fibroblasts has been demonstrated (33). Moreover, TGF-β type I and II receptor levels correlated with elevated collagen α2 (I) mRNA and promoter activity (33). TGF-β, acting through the Smad signaling pathway, regulates the expression of the key proteins that contribute to the pathogenesis of fibrosis. Specifically, Smad 3 is a key intercellular signal transduction molecule downstream of bleomycin-induced TGF-β1 action on skin fibroblasts, as supported by studies in Smad3 knockout mice (34). Activation of Smad 3 is a positive regulator of TGF-β signaling and Smad 2/3 nuclear translocation. Phosphorylation of Smad 3 is the hallmark of activated TGF-β signaling in lesional fibroblasts of bleomycin-induced scleroderma (22). In vitro studies using fibroblasts derived from either Smad 2- or 3-null embryos have revealed a complex picture of TGF-β1 transcriptional regulation, indicating distinct mechanisms of TGF-β1 gene regulation by Smad 2, Smad 3, or both (34). On keratinocytes, LPA-signaling leads to a functional activation of the TGF-β signal transducer Smad (35). In the present study, numbers of phospho-Smad 2/3+ cells and TGF-β1 mRNA expression were observed to be decreased in the skin treated with Ki16425 in bleomycin-induced mice (Fig. 4-5). This effect was associated with a decrease of collagen contents and TGF-β1 concentration as well as a downregulation of mRNA levels of CTGF and collagen α1 (I) in skin tissues. These results corresponded to a previous report of Ki16425 injection subcutaneously for murine renal fibrosis (16) in which transcriptional activity of fibrogenic cytokines such as CTGF and TGF-β was

decreased by $LPA_{1,3}$ receptor antagonist treatment as well as collagen synthesis. Moreover, myofibroblasts treated with LPA and TGF-β1 produced an additive effect on CTGF expression. CTGF induction in response to LPA requires the activation of c-jun N-terminal kinase (JNK), but not extracellular signal-regulated kinase (ERK) and Smad-2/3 phosphorylation or nuclear translocation, signaling pathways (36). Our data demonstrated that upon co-injection of bleomycin and $LPA_{1,3}$ receptor antagonist, a transient decrease in active TGF-β1 protein expression preceded that of CTGF mRNA expression and paralleled that of collagen α1 (I) mRNA. These results suggest that $LPA_{1,3}$ receptor antagonist decreases TGF-β through Smad signaling pathways and CTGF through the JNK signaling pathway in murine SSc induced by bleomycin. In addition, some studies have shown that IFN-γ, one of the Th1 cytokines, has an antifibrotic effect on scleroderma induced by bleomycin (37). LPA on matured dendritic cells enhances T-cell proliferation and increases the production of IFN-γ (38), which may shift Th2 cytokine balance to Th1 response. In this study, we showed that $LPA_{1,3}$ receptor inhibition decreased IFN-γ mRNA expression (Fig. 5). This result indicates that antifibrotic effects through the LPA signaling pathway occur despite blocking IFN-γ in the bleomycin-induced mice.

Myofibroblasts are characterized by α-SMA expression and into cytoskeletal stress fibers and play a major role in the pathogenesis of scleroderma (39). They also secrete increased amounts of extracellular matrix components, including collagen (40). Myofibroblasts predominate in areas of increased collagen deposition in scleroderma lesional skin, where the number of myofibroblasts correlates with the severity of fibrosis (41) and α-SMA-positive myofibroblasts are increased in the experimental mouse model of bleomycin-induced scleroderma (42). Promotion of myofibroblast

accumulation by LPA_1 signaling would therefore be expected to promote dermal fibrosis. LPA mediates multiple fibroblast activities that lead to the accumulation of these cells, including their recruitment and proliferation, and the prevention of their apoptosis (43). $LPA_{1,3}$ receptor antagonist Ki16425 decreased the proliferation of α-SMA-positive myofibroblasts induced by bleomycin on the dermis in mice. LPA_1 receptors are expressed on fibroblasts in SSc skin and showed a significant increase of LPA-activated chloride channel current activity (12). Therefore, antifibrotic effects of this agonist may result from the direct action of Ki16425 through a process such as transformation of fibroblasts into myofibroblasts.

Mast cells are increased in the skin of SSc (44) and bleomycin-induced mice (45). Several lines of evidence have shed light on local mast cell function in scleroderma pathology. Mast cells are one of the major sources of TGF-β in SSc, and release mediators or cytokines may play a role in accelerating formation of dermal sclerosis for stimulating fibroblasts to produce collagen in bleomycin-induced mice (45, 46). Yamamoto, et al. reported that after injection of bleomycin into mouse skin, infiltrating mast cells increased not only in the early edematous skin but also in the sclerotic skin and reached a peak at two to three weeks after the injection (47). In the present study, $LPA_{1,3}$ receptor antagonist significantly inhibited mast cell infiltration in the dermis of the bleomycin-induced SSc model. LPA accelerates the proliferation of human mast cells (48) and induces histamine release in mice via LPA_1 and/or LPA_3 receptors (49). Our results suggest that LPA receptor inhibition could mediate direct or indirect decreases on mast cell proliferation and contributes to the suppression of tissue fibrosis in the SSc model. Such characteristic responses of local mast cells differ considerably from the time-dependent regulation of active TGF-β1 protein, and more critically, the

past another study suggests that bleomycin-induced skin sclerosis was demonstrable in the mast cell–deficient strain of WBB6F1-W/Wv mice (50) and genetic ablation mice (51), such the same as was observed in control mice. These observations concerning local mast cell biology may provide insight into the as-yet uncharacterized action of bleomycin in the skin as well as the underlying conclusion that mast cells may not be the principal players in the establishment of bleomycin-induced scleroderma.

In conclusion, in this study, we demonstrated the therapeutic potential of *in vivo* $LPA_{1,3}$ receptor antagonist administration in the scleroderma model mouse, focusing on skin and lung sclerosis. Our data warrant further detailed investigations to clarify the disease stage–specific action of this multifactorial cytokine in scleroderma, particularly in respect to an adequate period of $LPA_{1,3}$ receptor antagonist administration to the lesional skin. Future studies are necessary to investigate the pathogenesis which $LPA_{1,3}$ receptor antagonist inhibits lung fibrosis, and determine the effect of *in vitro* $LPA_{1,3}$ receptor antagonist in scleroderma.

Acknowledgments

We are grateful to Tomoko Okada and Naoko Suzuki for their technical supports. All experimental procedures owing to animal study were approved by the Animal Care Committee of Fukushima Medical University on July 29, 2013 (No. 25090).

Author contributions

T. Ohashi performed the research and T. Yamamoto designed the research study. T. Ohashi, T. Yamamoto analysed the data and wrote the paper. All authors substantially contributed to the research study and were involved in drafting the article or revising it

critically, and all authors approved the submitted and final versions.

Conflicts of interest

The authors have declared no conflict of interests.

References

1 Varga J, Abraham D. J Clin Invest 2007: **117**: 557-567.

2 Querfeld C, Eckes B, Huerkamp C *et al*. J Dermatol Sci 1999: **21**: 13-22.

3 Chujo S, Shirasaki F, Kondo-Miyazaki M *et al*. J Cell Physiol 2009: **220**: 189-195.

4 Gailit J, Marchese MJ, Kew RR *et al*. J Invest Dermatol 2001: **117**: 1113-1119.

5 O'Reilly S, Hügle T, van Laar JM *et al*. Rheumatology (Oxford) 2012: **51**: 1540-1549.

6 Truchetet ME, Brembilla NC, Montanari E *et al*. Arthritis Rheum 2013: **65**: 1347-1356.

7 Pattanaik D, Postlethwaite AE. Discov Med 2010: **10**: 161-167.

8 Alexander SP, Mathie A, Peters JA. Br J Pharmacol 2011: **158 (Suppl.1)**: S1-254.

9 Williams JR, Khandoga AL, Goyal P *et al*. J Biol Chem 2009: **284**: 17304-17319.

10 Aoki J. Semin Cell Dev Biol 2004: **15**: 477-489.

11 Tokumura A, Carbone LD, Yoshioka Y *et al*. Int J Med Sci 2009: **6**: 168-176.

12 Yin Z, Carbone LD, Gotoh M *et al*. Rheumatology (Oxford) 2010: **49**: 2290-2297.

13 Castelino FV, Seiders J, Bain G *et al*. Arthritis Rheum 2011: **63**: 1405-1415.

14 Tager AM, LaCamera P, Shea BS *et al*. Nat Med 2008: **14**: 45-54.

15 Watanabe N, Ikeda H, Nakamura K *et al*. Life Sci 2007: **81**: 1009-1015.

16 Pradère JP, Klein J, Grès S *et al*. J Am Soc Nephrol 2007: **18**: 3110-3118.

17 Pradère JP, Gonzalez J, Klein J *et al*. Biochim Biophys Acta 2008: **1781**: 582-587.

18 Yamamoto T, Takagawa S, Katayama I *et al*. J Invest Dermatol 1999: **112**: 456-462.

19 Yoshizaki A, Yanaba K, Yoshizaki A *et al*. Arthritis Rheum 2010: **62**: 2476-2487.

20 Wu M, Varga J. Curr Rheumatol Rep 2008: **10**: 173-182.

21 Whitfield ML, Finalay DR, Murray JI *et al*. Proc Natl Acad Sci U S A 2003: **100**: 12319-12324.

22 Takagawa S, Lakos G, Mori Y *et al*. J Invest Dermatol 2003: **121**: 41-50.

23 Mori Y, Hinchcliff M, Wu M *et al*. Exp Cell Res 2008: **314**: 1094-1104.

24 Ashcroft T, Simpson JM, Timbrell V. J Clin Pathol 1988: **41**: 467-70

25 Mazereeuw-Hautier J, Gres S, Fanguin M *et al*. J Invest Dermatol 2005: **125**: 421-427.

26 Demoyer JS, Skalak TC, Durieux ME. Wound Repair Regen 2000: **8**: 530-537.

27 Evans RA, Tian YC, Steadman R *et al*. Exp Cell Res. 2003: **282**: 90-100.

28 Nicolás FJ, De Bosscher K, Schmierer B *et al*. J Cell Sci 2004: **117**: 4113-4125.

29 Mori Y, Chen SJ, Varga J. Arthritis Rheum 2003: **48**: 1964-1978.

30 Denton CP, Abraham DJ. Curr Opin Rheumatol 2001: **13**: 505-511.

31 Yamamoto T, Takagawa S, Katayama I *et al*. Clin Immunol 1999: **92**: 6-13.

32 Zhu H, Bona C, McGaha TL. Autoimmunity 2004: **37**: 51-55.

33 Kawakami T, Ihn H, Xu W *et al*. J Invest Dermatol 1998: **110**: 47-51.

34 Lakos G, Takagawa S, Chen SJ *et al*. Am J Pathol 2004: **165**: 203-217.

35 Sauer B, Vogler R, Zimmermann K *et al*. J Invest Dermatol 2004: **123**: 840-849.

36 Cabello-Verrugio C, Córdova G, Vial C *et al*. Cell Signal 2011: **23**: 449-457.

37 Yamamoto T, Takagawa S, Kuroda M *et al*. Arch Dermatol Res 2000: **292**: 362-365.

38 Chen R, Roman J, Guo J, West E *et al*. Stem Cells Dev 2006: **15**: 797-804.

39 Jelaska A, Korn JH. Arthritis Rheum 2000: **43**: 2230-2239.

40 Hinz B, Gabbiani G. Thromb Haemost 2003: **90**: 993-1002.

41 Kissin EY, Merkel PA, Lafyatis R. Arthritis Rheum 2006: **54**: 3655-3660.

42 Yamamoto T, Nishioka K. Clin Immunol 2002: **102**: 77-83.

43 Fang X, Yu S, LaPushin R *et al*. Biochem J 2000: **352**: 135-143.

44 Seibold JR, Giorno RC, Claman HN. Arthritis Rheum 1990: **33**: 1702-1709.

45 Yamamoto T, Takahashi Y, Takagawa S *et al*. J Rheumatol 1999: **26**: 2628-2634.

46 Ozbilgin MK, Inan S. Clin Rheumatol 2003: **22**: 189-195.

47 Yamamoto T. Arch Dermatol Res 2006: **297**: 333-344.

48 Bagga S, Price KS, Lin DA *et al*. Blood 2004: **104**: 4080-4087.

49 Hashimoto T, Ohata H, Honda K. J Pharmacol Sci 2006: **100**: 82-87.

50 Yamamoto T, Takagawa S, Nishioka K. Arch Dermatol Res 2001: **293**: 532-536.

51 Willenborg S, Eckes B, Brinckmann J **et al**. J Invest Dermatol 2014: **134**: 2005-2015.

Example Table (would be referenced in Materials and methods section rather than listing the primers there):

Table 1. **Primers used in this study**

	Sense	Antisense
TGF-β1	5′-TTTCCGCTGTGCTACTGCAAGTC-3′	3′-AGGGCTGTCTGGAGTCCTCA-5′
CTGF	5′-ACCCGAGTTACCAATGACAATACC-3′	3′-CCGCAGAACTTAGCCCTGTATG-5′
MIP-1α	5′-CATGACACTCTGCAACCAAGTCTTC-3′	3′-ACTTTGGTCGTCGGAAACGAG-5′
IFN-γ	5′-TGACGGGAGCACCTGTTACAC-3′	3′-GATGTATGATTTGTATGCCAGCTTT-5′
TNF-α	5′-CAACGGCACCGTGACAATC-3′	3′-TCACATCATTCAACACGGATGGAGG-5′
collagen α1(I)	5′-CAGGGTATTGCTGGACA-3′	3′-GGACCTTGTTTGCCAGGTTCA-5′
GAPDH	5′-TGTGTCCGTCGTGGATCTGA-3′	3′-TTGCTGTTGAAGAAGTCGCAGGAG-5′

Figures

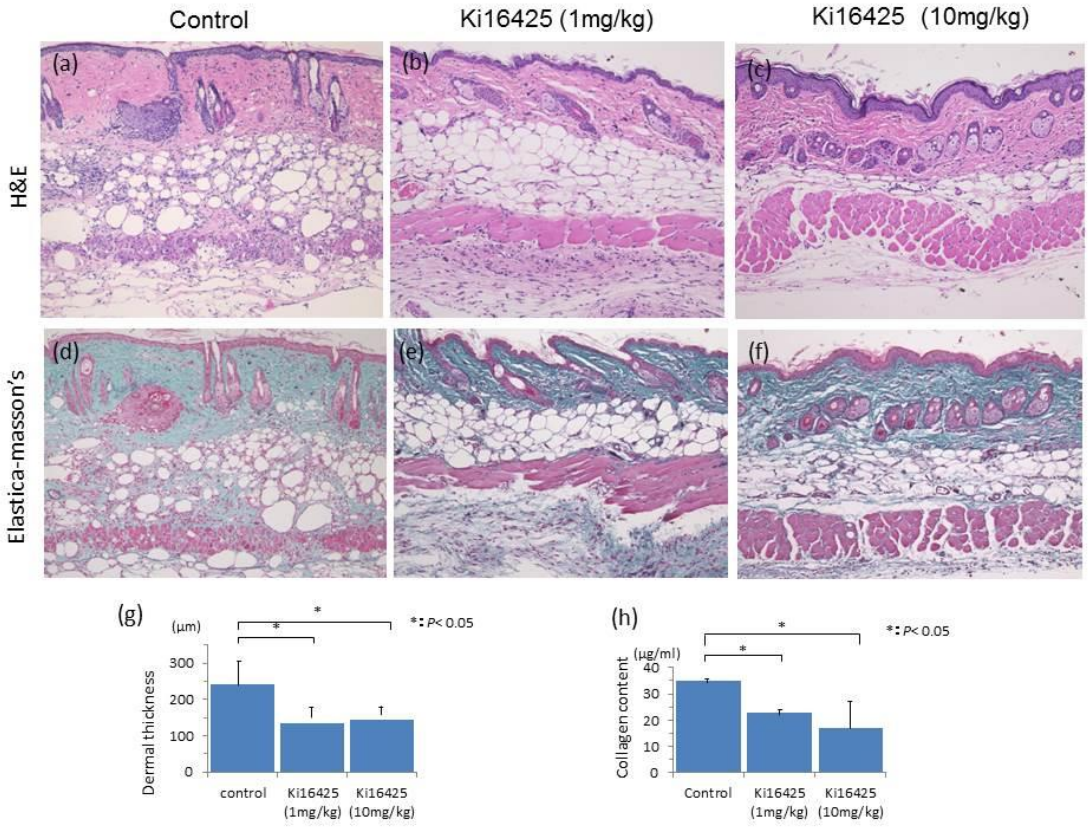

Figure 1. Histopathological evaluation of the skin of bleomycin induced mice treated with (a, d) oil, (b, e) Ki16425 (1 mg/kg) , (c, f) Ki16425 (10 mg/kg) for 4 weeks by H&E (a-c) and Elastica-masson's staining (d-f). Magnification × 100. (g) Dermal thickness measured in 10 locations/HPF, in 10HPF/skin sample, *$p < 0.05$, control mice vs. Ki16425-treated mice, n = 5 mice per group (1, 10 mg/kg). The dermal thickness of Ki16425-treated mice was reduced compared with that of oil-treated control mice. There was no statistically significant dose dependency of inhibition in the Ki16425 treatment group. (h) The hydroxyproline content of injected skin sites. The hydroxyproline content of local skin sites co-injected. *$P < 0.05$, control mice vs. Ki16425-treated mice, n = 5 mice per group (1, 10 mg/kg).

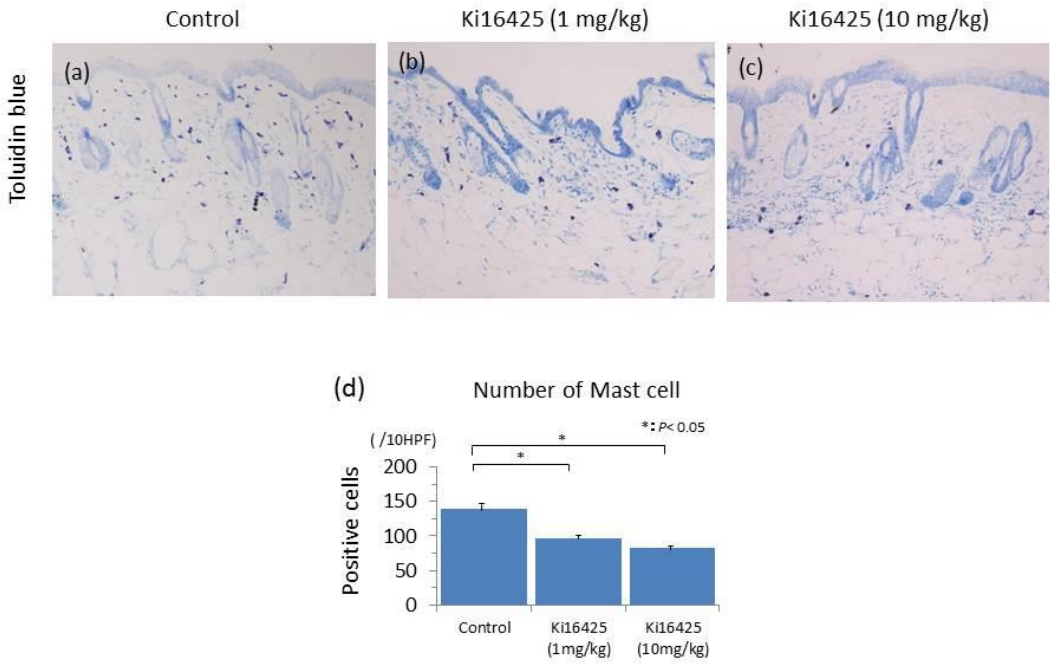

Figure 2. Toluidine blue staining showing mast cell infiltration after bleomycin injection and Ki16425 treatment. (a) Dermal infiltration of mast cells after injection of bleomycin and oil for 4 weeks as a control. (b, c) Histopathological changes in mast cell infiltration. Ki16425-terated group showed a decrease compared with control group. (d) Dermal mast cell number. Dermal mast cell number was decreased in the Ki16425 treatment group. Numbers of mast cell were measured in 10 locations/HPF, in 10 HPF/skin sample, $*p < 0.05$, control mice vs. Ki16425-treated mice (1, 10 mg/kg), n = 5 mice per group. However, there was no significant dose dependency of inhibition in the Ki16425 treatment group.

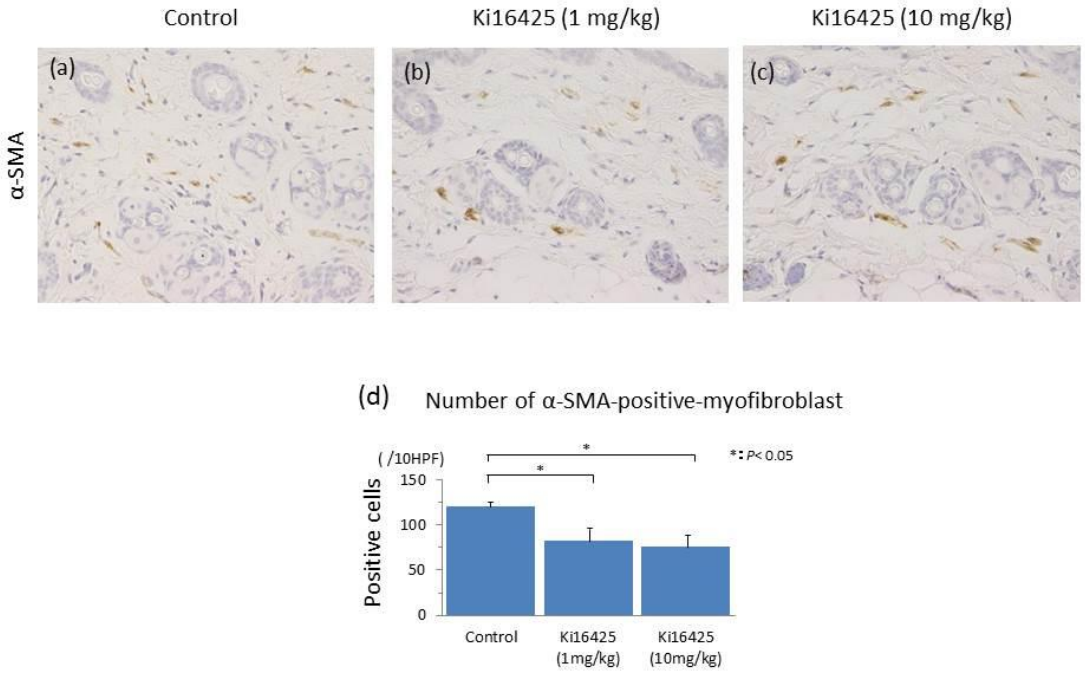

Figure 3. Diminished accumulation of α-smoooth muscle actin (α-SMA)-positive myofibroblasts in the dermis of bleomycin-induced mice treated with (a) oil, (b) Ki16425 (1 mg/kg), (c) Ki16425 (10 mg/kg). Original magnification × 400. (d) Quantification of α-SMA+ myofibroblasts in the dermis of mice injected with bleomycin. Numbers of α-SMA+ cell were decreased in the Ki16425 treatment group. Numbers of α-SMA+ cell were measured in 10 locations/HPF, in 10 HPF/skin sample, *p<0.05, control mice vs. Ki16425-treated mice (1, 10 mg/kg), n = 5 mice per group. The difference between both mice treated with dose of Ki16452 was not significant.

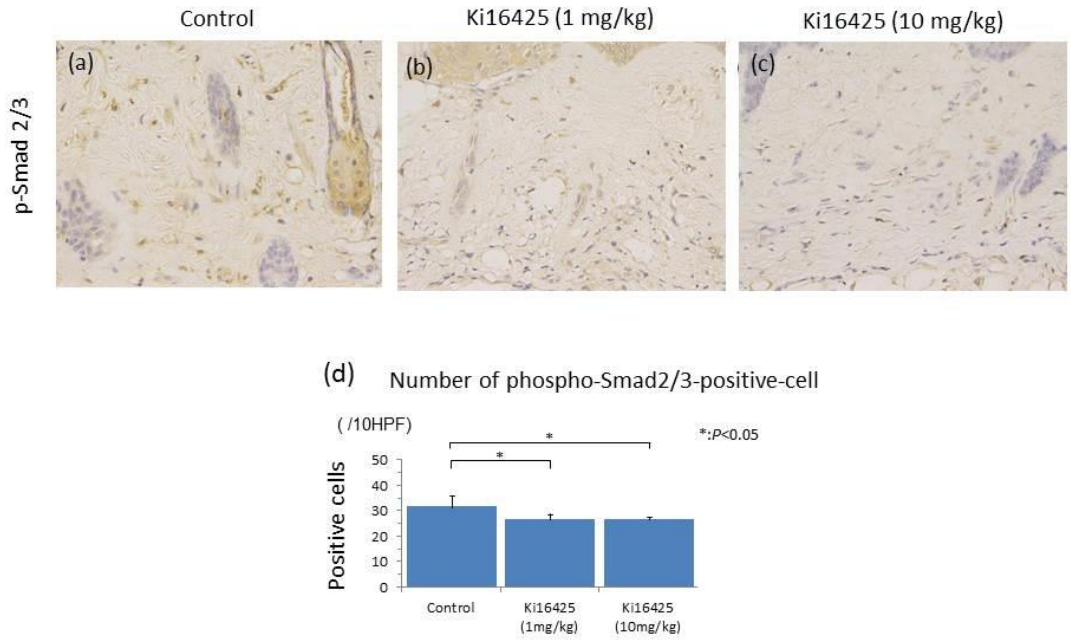

Figure 4. Diminished accumulation of phospho-Smad 2/3 (p-Smad 2/3)-positive myofibroblasts in the dermis of bleomycin-induced mice treated with (a) oil, (b) Ki16425 (1 mg/kg), or (c) Ki16425 (10 mg/kg). Original magnification × 400. (d) Quantification of p-Smad 2/3+ cells in the dermis of mice injected with bleomycin. Numbers of p-Smad 2/3+ cells were decreased in the Ki16425 treatment group. Numbers of p-Smad 2/3+ cell were measured in 10 locations/HPF, in 10 HPF/skin sample, *p<0.05, control mice vs. Ki16425-treated mice (1, 10 mg/kg), n = 5 mice per group. The difference between both mice treated with dose of Ki16452 was not significant.

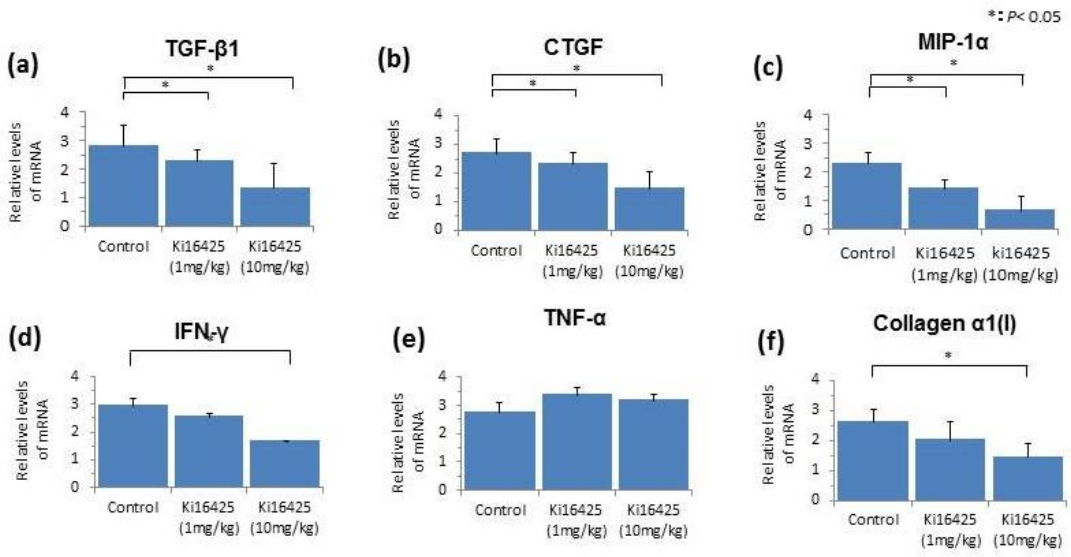

Figure 5. Expression of fibrogenic cytokines and collagenα1 (I) mRNA were analysed by a real-time PCR asssy ;(a) TGF-β1, (b) CTGF, (c) MIP-1α, (d) IFN-γ, (e) TNF-α, and (f) collagen α1 (I). K16425 (10 mg/kg) treatment significantly reduced TGF-β1, CTGF, MIP-1α, IFN-γ, and collagen α1 (I) mRNA expression compared with the oil as a control, n = 3 mice per group. Ki16245 (1 mg/kg) treatment reduced TGF-β1, CTGF, and MIP-1α mRNA expression compared with the oil as a control, n = 3 mice per group. There was no statistically significant difference in TNF-α mRNA expression levels between the control and Ki16425-treated groups.

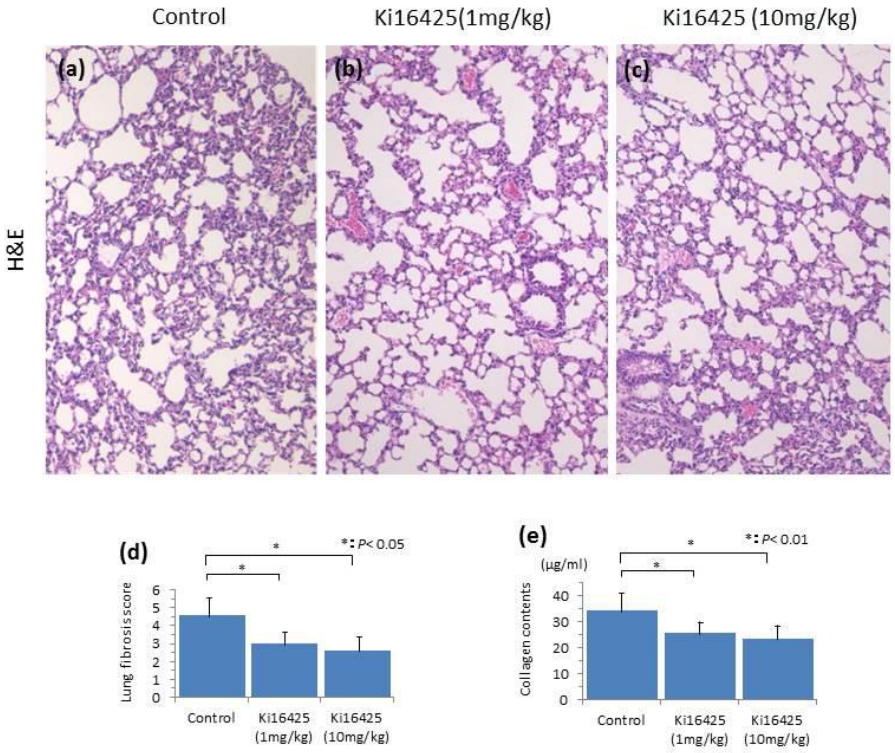

Figure 6. Histopathological evaluation of the lung of bleomycin induced mice treated with (a) oil, (b) Ki16425 (1 mg/kg), (c) Ki16425 (10 mg/kg) for 4 weeks by H&E staining. Magnification × 100. (d) The score of lung fibrosis. The lung fibrosis score of Ki16425-treated mice was reduced compared with that of oil-treated control mice, n = 7 mice per group. There was no statistically significant dose dependency of inhibition in the Ki16425 treatment group. (e) The hydroxyproline content of lung tissue.